

Shaped nondiffracting beams

Carlos López-Mariscal^{1,2,*} and Kristian Helmersen¹

¹National Institute of Standards and Technology, Gaithersburg, Maryland 20899-8424, USA

²Photonics and Mathematical Optics Group, Tecnológico de Monterrey, Monterrey 64849, Mexico

*Corresponding author: clopez@nist.gov

Received November 9, 2009; revised January 31, 2010; accepted March 7, 2010;
posted March 11, 2010 (Doc. ID 119584); published April 15, 2010

We demonstrate that nondiffracting beams can be generated with an arbitrary transverse shape. In particular, we show that the azimuthal complex modulation of the angular spectra of Helmholtz–Gauss wave fields constitutes a degree of freedom sufficient to tailor nondiffracting beams with an intensity pattern of choice.

© 2010 Optical Society of America

OCIS codes: 020.3320, 070.6120, 100.5070, 220.3740.

Nondiffracting beams (NDBs) are unique in that they propagate while preserving their integrity [1], an ability that has resulted in their widespread use in applied science. The best known example of this class of wave fields, the Bessel beam, has been successfully used in optical manipulation [2], biophotonics [3], optical interconnects [4,5], and optical coherence tomography [6], where it is particularly advantageous in comparison to a conventional Gaussian beam owing to its comparatively longer invariance length.

In this Letter, we show that NDBs with a transverse intensity pattern of choice can be produced. In particular, we prospect the complex space of the angular spectrum in search for a two-dimensional (2D) complex modulation that corresponds to a beam with the desired transverse intensity profile and at the same time, is an NDB. The results shown here broaden the applications of NDBs by providing with a means of tailoring their transverse shape.

NDBs have a transverse structure independent of the longitudinal coordinate. They can be regarded as the outcome of the interference of the set of plane waves with constant inclination θ_0 in reciprocal space, as shown in Fig. 1. The ends of the constituting wave vectors lie on an infinitely thin ring of radius k_t that corresponds to the transverse spatial frequency,

$$k_t = \frac{2\pi}{\lambda} \sin \theta_0. \quad (1)$$

As a consequence of their wave vector distribution, the central portion of the transverse intensity of NDBs remains invariant along an extended propagation distance z_{\max} , which can be larger than the Rayleigh range z_R of a Gaussian beam of comparable transverse extent. A physically consistent representation of NDBs is provided by the formalism of Helmholtz–Gauss (HzG) beams [7]. The functional form of HzG beams,

$$U(\mathbf{r}) = \exp\left(-i\frac{k_t^2 z}{2k\mu}\right) G(\mathbf{r}) W(\mathbf{r}_t), \quad (2)$$

incorporates the product of the Gaussian envelope,

$$G(\mathbf{r}) = \frac{\exp(ikz)}{\mu} \exp\left(-\frac{r^2}{\mu w_0^2}\right), \quad (3)$$

with waist size w_0 , and the transverse shape of a NDB $W(\mathbf{r}_t)$. Here, $\mu = 1 - iz/z_R$, $z_R = kw_0^2/2$, and \mathbf{r}_t is the transverse coordinate. The intensity of an HzG beam does not vary significantly along a length $z_{\max} = z_R/\gamma$ measured from its waist, where $\gamma = \frac{1}{2}k_t w_0$ is the ratio of the inclination angle θ_0 and the spread of the Gaussian function. The angular spectrum of HzG beams, given by the 2D Fourier transform [8] $\mathcal{F}\{U(\mathbf{r})\} = \tilde{U}(u, v; z)$, is characterized by a support $\|\tilde{U}(u, v; z)\|$ of annular shape in reciprocal space, as shown in Fig. 1(b). The functional form of the spectrum is given by

$$\tilde{U}(u, v; z) = D(z) \exp\left(-\frac{\omega_0^2 \mu}{4} \rho^2\right) W\left(\frac{\omega_0^2}{2i} u, \frac{\omega_0^2}{2i} v; k_t\right), \quad (4)$$

where $k_t^2 = u^2 + v^2$ and

$$D(z) = \frac{\omega_0^2}{2} \exp\left(\frac{1}{4} k_t^2 \omega_0^2\right) \exp(ikz). \quad (5)$$

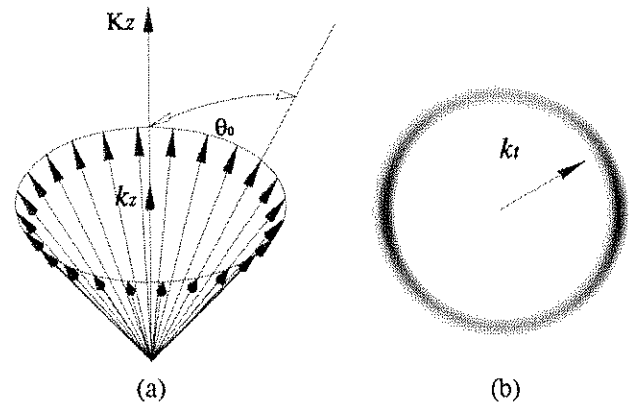


Fig. 1. (a) Wave-vector distribution of NDBs. In reciprocal space, the wave vectors lie on the surface of a cone with semiangle θ_0 and end in a circular ring with radius k_t . (b) Typical power spectrum of an HzG beam. Notice the annular-shaped support and associated radial frequency content.

Although the specific shape of the support of NDBs is responsible for their extended propagation invariance length, it is the complex angular modulation of their angular spectra that determines the specific transverse profile of the beams. A random modulation of the spectrum in the azimuthal coordinate, for example, results in a beam with random, invariant transverse intensity and extended propagation distance [9]. The modulation of the complex amplitude of the angular spectrum therefore represents a degree of freedom that can be used to sculpt a desired transverse shape onto an NDB. Finding the corresponding complex modulation allows the generation of NDBs with the intensity profile of choice.

In our experiments, we have chosen an arbitrary intensity pattern $I_0(\mathbf{r}_t) = U_0(\mathbf{r}_t)^2$ and have searched for a solution for the corresponding complex modulation in Fourier space with the constraint of an annular support, which is the defining characteristic of all NDBs. In particular, we probe the space of angular spectra with a modified adaptive additive phase algorithm [10] that incorporates the functional form of the support as a spectral constraint. We have encoded the complex modulation in a phase-only computer-generated hologram (CGH) by means of a spatial light modulator (SLM) addressable with a super video graphics array (SVGA) signal with a resolution of 800×600 pixels. Figures 2(a) and 2(b) show the desired intensity profile $I_0(\mathbf{r}_t)$ and the numerical

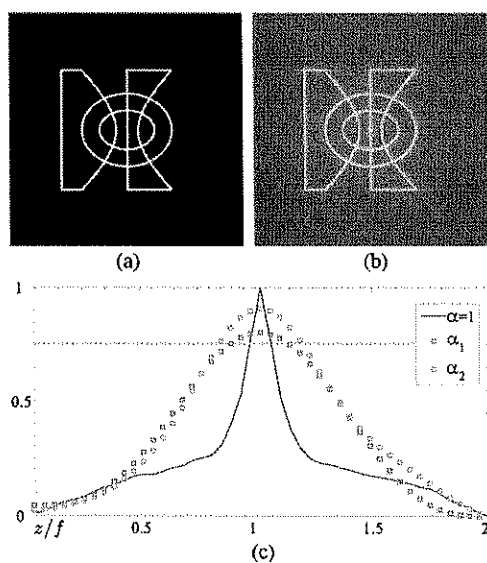


Fig. 2. (Color online) (a) The desired transverse intensity, $I_0(\mathbf{r}_t)$ and (b) its simulated intensity profile (log scale) from the numerical reconstruction of the CGH with a Fourier lens of focal length $f=0.4$ m at $z=f$. (c) Normalized cross-correlation coefficient for different beams and the desired transverse intensity as a function of propagation distance. The red squares and blue circles correspond to relative space-bandwidth products $\alpha_1=0.34$ and $\alpha_2=0.78$, respectively. The black line represents the case of no frequency constraints and the dashed green line corresponds to $m=0.75$ for reference. Note that the ranges of z/f for which $m > 0.75$ in each case are roughly four ($z_{\max}=0.26$ m) and three times ($z_{\max}=0.18$ m) larger than for a beam without the support constraints, respectively.

reconstruction of the CGH, $I_R(\mathbf{r}_t)$, respectively. Typical values for the signal-to-noise ratio are +11 dB. We use a Gaussian beam to illuminate the CGH; the residual available bandwidth of the SLM is filled with an encoded checkerboard pattern to avoid a zeroth-order contribution at the Fourier plane. In an application, where optical power is limited, illuminating the CGH with an annular beam shaped with an axicon, for example, yields a higher insertion efficiency of the CGH.

Figure 2(c) shows the normalized cross-correlation m of $I_0(\mathbf{r}_t)$ and $I_R(\mathbf{r}_t)$ as a function of the longitudinal distance. The squares and circles correspond to two different instances of spectra with relative space-bandwidth products α_1 and α_2 , respectively, while the value for a CGH with no spatial constraints is given by the continuous black line for reference. As expected, m is maximum at the Fourier plane $z=f$ in all cases. However, for NDBs, m has a higher value for longer distances, an evidence of their extended focal depths. While using a narrower spectrum allows for a longer depth of focus, the reduced set of spatial frequencies that can be encoded results in comparably lower values of m at the focal plane.

Constraining the support constitutes a bandpass filter operation, which selectively eliminates of spatial frequencies and in turn yields lower values of m . Such frequency discrimination leads in turn to extended propagation distances at the cost of significant bandwidth loss. The annular bounds of the angular spectrum of NDBs effectively reduce the space-bandwidth product of the wave field, a situation that is desirable where a reduction of high-frequency noise is an advantage and sacrificial bandwidth is available. For instance, the use of spectral constraints has been previously explored in connection with the performance of coherent light diffusers featuring reduced speckle [11]. In this case, the average size of the speckles can be reportedly controlled by modifying the values of the frequency constraints.

Figure 3(a) corresponds to the beam transverse intensity profile at the Fourier plane and at a distance $z=z_{\max}$ (insert), defined as the axial point where the value of m drops below 0.75. Notice that the beam

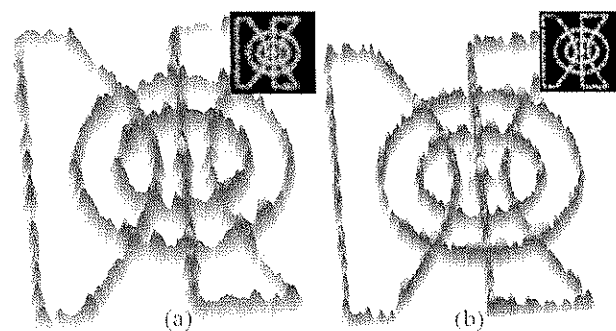


Fig. 3. (Color online) (a) Numerical simulation of the beam profile $I_0(\mathbf{r}_t)$ at $z=f$ and at $z=z_{\max}$ and (b) experimental beam profile $I_R(\mathbf{r}_t)$ reconstructed from the CGH with $f=0.40$ m. In both cases $\alpha=0.34$. Gaussian spread takes over after the beams propagate for a distance $z_{\max} \gg z_R$, as expected from an HzG beam.

preserves its general shape until Gaussian spread takes over after $z=z_{\max}$. The experimental reconstruction using the same parameters is shown in Fig. 3(b), where the spread predicted by Fig. 3(a) is evident. Noticeably, a beam with a higher space-bandwidth product yields a higher fidelity in virtue of the inclusion of a broader range of spatial frequencies. However, its intensity profile degrades significantly after a shorter propagation distance in comparison with its band-limited counterpart, as shown in Fig. 2(c).

In conclusion, we have produced NDBs with arbitrary intensity profiles by calculating their corresponding complex spectra with the support constraints of HzG beams. Moreover, we have experimentally verified the propagation properties of the produced beams throughout an extended invariance distance, and we have quantitatively assessed the fidelity of the beams compared to the intended intensity distribution for different sets of constraints. Our results open new avenues in the use of NDBs by introducing a means to control their transverse profile and are currently being extended to the recently demonstrated accelerating beams [12,13].

The authors wish to acknowledge fruitful discussions with J. C. Gutiérrez-Vega and S. Lopez-Aguayo, from Tecnológico de Monterrey, Mexico and with F. M. Dickey from FMD Consulting, LLC.

References

1. J. Durnin, J. J. Miceli, and J. H. Eberly, *Phys. Rev. Lett.* **58**, 1499 (1987).
2. V. Garcés-Chávez, D. McGloin, H. Melville, W. Sibbett, and K. Dholakia, *Nature* **419**, 145 (2002).
3. X. Tsampoula, V. Garcés-Chávez, M. Comrie, D. Stevenson, M. B. Agate, F. J. Gunn-Moore, C. T. A. Brown, and K. Dholakia, *Appl. Phys. Lett.* **91**, 053902 (2007).
4. C. Yu, M. R. Wang, A. J. Varella, and B. Chen, *Opt. Commun.* **177**, 369 (2000).
5. R. P. MacDonald, S. A. Boothroyd, T. Okamoto, J. Chrostowski, and B. A. Syrett, *Opt. Commun.* **122**, 169 (1996).
6. Z. Ding, H. Ren, Y. Zhao, J. S. Nelson, and Z. Chen, *Opt. Lett.* **27**, 243 (2002).
7. J. C. Gutiérrez-Vega and M. A. Bandres, *J. Opt. Soc. Am. A Opt. Image Sci. Vis.* **22**, 289 (2005).
8. This reduces to the Fourier-Bessel transform, also called a Hankel transform, for azimuthally symmetric fields.
9. D. M. Cottrell, J. M. Craven, and J. A. Davis, *Opt. Lett.* **32**, 298 (2007).
10. J. E. Curtis, B. A. Koss, and D. G. Grier, *Opt. Commun.* **207**, 169 (2002).
11. R. Brauer, F. Wyrowsky, and O. Byngdahl, *J. Opt. Soc. Am. A* **8**, 572 (1991).
12. M. V. Berry and N. L. Balazs, *Am. J. Phys.* **47**, 264 (1979).
13. G. A. Siviloglou, J. Broky, A. Dogariu, and D. N. Christodoulides, *Phys. Rev. Lett.* **99**, 213901-1 (2007).